Structural Engineering and Mechanics, Vol. 6, No. 2 (1998) 125-141
DOI: http://dx.doi.org/10.12989/sem.1998.6.2.125

System seismic performance of haunch repaired steel MRFs: dual panel zone modeling and a case study

Cheol Ho Lee†

Department of Architectural Engineering, College of Engineering, Kyungnam University, Masan, Kyungnam 631-701, Korea

Abstract. Recent test results of steel moment connections repaired with a haunch on the bottom side of the beam have been shown to be a very promising solution to enhancing the seismic performance of steel moment-resisting frames. Yet, little is known about the effects of using such a repair scheme on the global seismic response of structures. When haunches are incorporated in a steel moment frame, the response prediction is complicated by the presence of "dual" panel zones. To investigate the effects of a repair on seismic performance, a case study was conducted for a 13-story steel frame damaged during the 1994 Northridge earthquake. It was assumed that only those locations with reported damage would be repaired with haunches. A new analytical modeling technique for the dual panel zone developed by the author was incorporated in the analysis. Modeling the dual panel zone was among the most significant consideration in the analyses. Both the inelastic static and dynamic analyses did not indicate detrimental side effects resulting from the repair. As a result of the increased strength in dual panel zones, yielding in these locations were eliminated and larger plastic rotation demand occurred in the beams next to the shallow end of the haunches. Nevertheless, the beam plastic rotation demand produced by the Sylmar record of 1994 Northridge earthquake was still limited to 0.017 radians. The repair resulted in a minor increase in earthquake energy input. In the original structure, the panel zones should dissipate about 80% (for the Oxnard record) and 70% (for the Sylmar record) of the absorbed energy, assuming no brittle failure of moment connections. After repair, the energy dissipated in the panel zones and beams were about equal.

Key words: steel moment-resisting frame; connection; dual panel zone; haunch; repair; seismic.

1. Introduction

The majority of damage observed in many steel moment-resisting frames (steel MRFs) after the 1994 Northridge earthquake has been local fractures at beam-to-column welded joints. Instead of assumed ductile response, brittle fracture was prevalent. In an effort to repair damaged steel moment frames as well as to strengthen existing and new steel construction after the Northridge earthquake, a variety of ideas have been proposed and verified experimentally. At the University of California, San Diego, four damaged full-scale size specimens were repaired by adding a haunch on the bottom side of the beam and tested either statically or dynamically (Uang and Bondad 1996a, 1996b). Fig. 1 shows the details of one specimen (Uang and Bondad 1996a). The test results in Fig. 2 clearly show the effectiveness of adding haunch to move the plastic hinge away from the column face and to reduce the stress demand in the groove welds.

Although a haunch-strengthened moment connection performed well at the subassembly level, the overall seismic performance of repaired structures and possible side effects arising from the

† Associate Professor

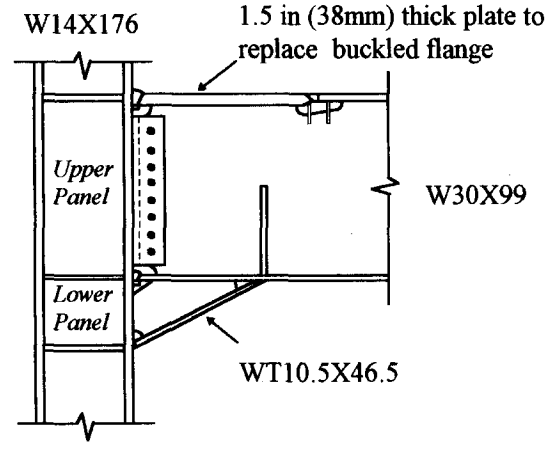

Fig. 1 A haunch repaired steel moment connection (Uang and Bondad 1996a).

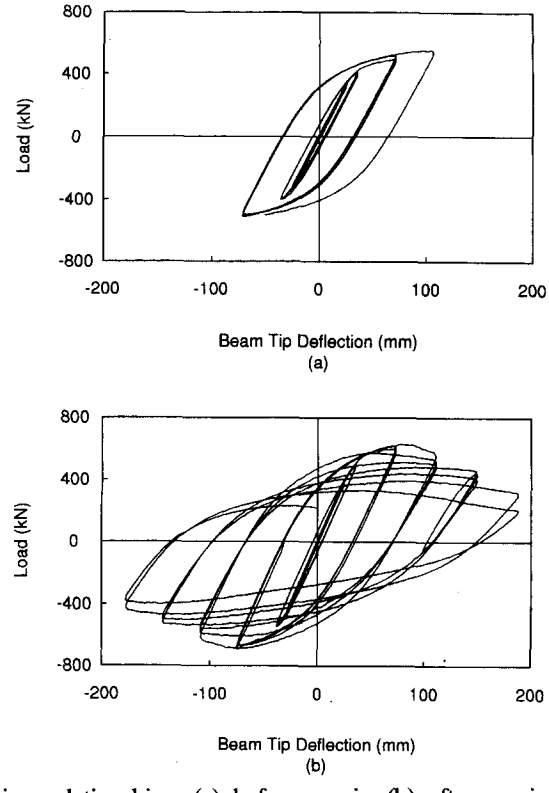

Fig. 2 Load versus tip deflection relationships: (a) before repair; (b) after repair (Uang and Bondad 1996a).

haunch reinforcement are not well understood. When haunches are incorporated in a steel moment frame, the response prediction is complicated by the presence of "dual" panel zones; the dual panel zone in a steel column is formed when the conventional beam-to-column connection in steel MRFs is enhanced for seismic performance by adding haunches on either or both sides of the column. Conventional modeling for the panel zone cannot be applied in this case and a new modeling technique is needed. The problem is complicated by the fact that several situation may

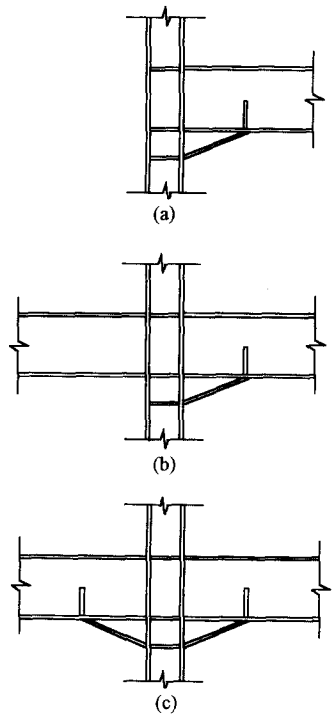

Fig. 3 Haunch reinforcenments on the bottom side of the beam: (a) exterior connection; (b) interior connecton (haunch on one side); (c) interior connection (haunches on both sides).

occur (see Fig. 3).

The main objective of this study is to answer some concerns regarding the use of haunches to reinforce existing structures at damaged locations. A case study was undertaken for a thirteen-story steel MRF building damaged during the 1994 Northridge earthquake. To this end, a new analytical modeling procedure for the panel zone with haunch reinforcement was incorporated in the analysis. As a result of modifying the structure with haunch, variations of the following are then investigated:

(1) dynamic characteristics and lateral stiffness,
(2) ultimate strength,
(3) yield mechanism, including the possibility of a weak story formation,
(4) story drift demand,
(5) distribution of plastic rotations and
(6) redistribution of energy dissipation in beams, panel zones, and columns.

2. Basis of repair design

Lateral resistance of the 13-story building was provided by a perimeter steel MRF (Fig. 4). Except for box corner columns, wide flange shapes of A36 steel were used for all other members (Fig. 5). The damage distribution of the frame along Line 4 in the N-S direction is shown in Fig. 6; approximately 25% of the connections failed in this frame. For a total of eighty-four connections in the frame, twenty-one locations were assumed to be repaired and reinforced with

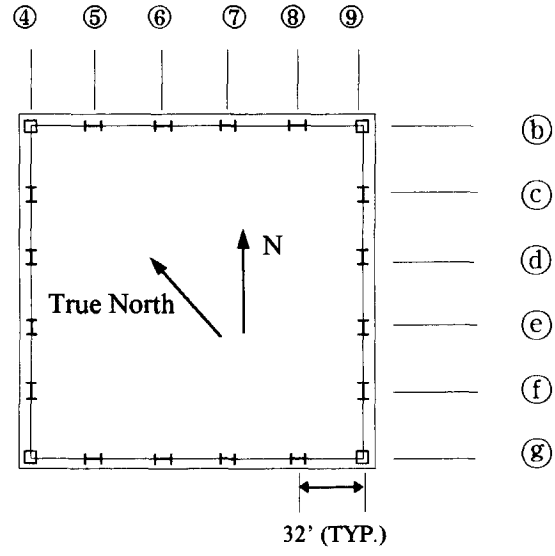

Fig. 4 Schematic plan.

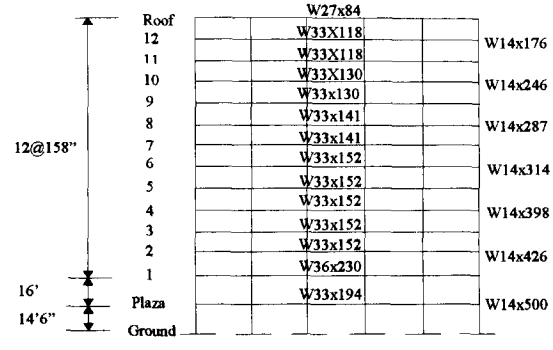

Fig. 5 Frame elevation and member size.

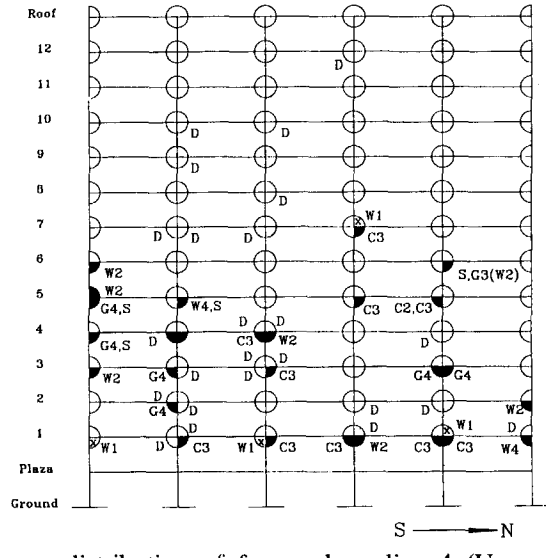

Fig. 6 Damage distribution of frame along line 4 (Uang, *et al.* 1995).

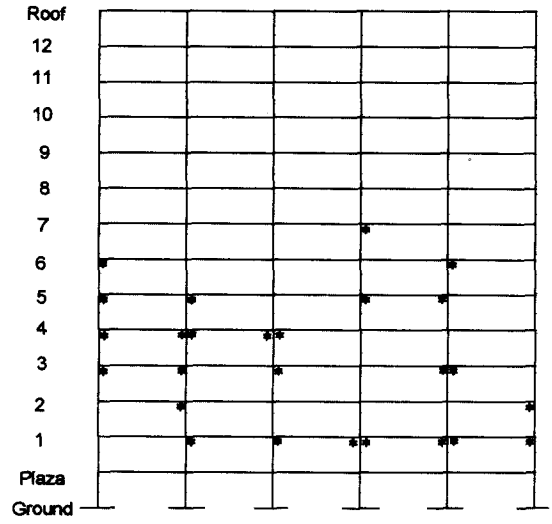

Fig. 7 Selected locations for reforcement with haunch.

haunches as shown in Fig. 7. The selection included the locations with flange weld damage, girder damage, and column flange damage. Refer to Uang, *et al.* (1995) for a detailed description of the building and damage types.

The proposed SAC Interim Guidelines (1995) were used to proportion haunches. The capacity design concept was adopted by the Guidelines, and the probable beam strength M_{pr} was computed to be

$$M_{pr} = 1.7 M_n \tag{1}$$

where M_n is the beam plastic moment for a nominal yield stress of 36 ksi, and an overstrength factor of 1.7 is used to reflect material overstrength and strain hardening. Structural shapes WT 18 of A572 Gr. 50 steel were used for haunch repair. In repair design it was assumed that beam plastic hinge would form at a distance $d_b/3$ away from the shallow end of the haunch, where d_b is the depth of the existing beam. The haunch depth and haunch angle were set equal to eighteen inches and thirty degrees, respectively. See Table 1 for the haunch shapes. The flexural strength of the reinforced joint at the face of the column was about twice that of the original steel beam.

Table 1 Selected sections and flexural stiffness coefficients of haunches

Floor (1)	WT Secton (2)	k_{ii} (3)	k_{jj} (4)	$k_{ij} = k_{ji}$ (5)
7	WT18×97	7.69	5.23	3.38
6	WT18×97	7.49	5.19	3.17
5	WT18×97	7.49	5.19	3.17
4	WT18×97	7.49	5.19	3.17
3	WT18×97	7.49	5.19	3.17
2	WT18×97	7.49	5.19	3.17
1	WT18×140	6.73	4.80	2.88

Note: haunch stiffiness matrix $[K] = \dfrac{EI_b}{L_b}\begin{bmatrix} k_{ii} & k_{ij} \\ k_{ji} & k_{jj} \end{bmatrix}$

3. Modeling of structure

3.1. Modeling assumptions

The computer program DRAIN-2DX (Prakash, *et al.* 1993) was used to perform both the inelastic static and dynamic analyses. A bare steel frame was used, without slab participation. Live load was not considered in assessing building reactive weight and partition load of 10 psf was included for seismic reactive mass calculation. The ground level was assumed as the fixed base and the plaza level was modeled with infinitely stiff springs to prevent rotation and translation. Gravity columns were ignored in the assessment of lateral resistance. The P-delta effect was considered by introducing a vertical line of fictitious columns linked to the moment-resisting frame. Rayleigh damping with 5% damping factor was assigned to the first and third modes. The first three modes took 94% of the total effective modal mass.

Beams and columns were modeled by the beam-column element (i.e., Element 2 of DRAIN-2DX). Expected yield strength for the AISC shape groups was adopted according to recent AISI study (1994). Thus, F_y of 47.3 ksi was used for the A36 beams and columns. Two percent strain hardening was assumed for the beams and columns. One hundred percent rigid-end offsets were considered at the end of beams and columns. For columns, the LRFD (AISC 1994) axial force versus moment interaction curve with the resistance factor set to one was used to model the yielding strength. The calculated flexural stiffness coefficients of the haunches are summarized in Table 1. They were modeled as a beam element of variable cross section.

A semi-rigid element (i.e., Element 4 of DRAIN-2DX) was used to model all the panel zones of interior connections, which had doubler plates of varying thickness along the height of the building. All the exterior connections were assumed to be rigid because box sections were used for the corner columns. Krawinkler's (1978) recommendation was used when a joint was not reinforced with haunch (refer to Fig. 8). When a connection is reinforced with haunch, Krawinkler's formulation cannot be applied. An analytical modeling procedure recently developed by the author (Lee and Uang 1995a, 1995b, 1997) was used for the dual panel zone. Due to space limitations, just a brief summary of the procedure is given in the following section.

3.2. Modeling of the dual panel zone

Treating the dual panel zone as a two-spring serial system in shear, and defining a secant

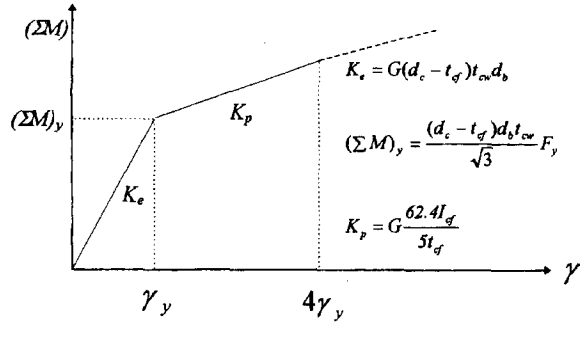

Fig. 8 Unbalanced beam moment versus average shear strain relationship (Krawinkler 1978).

shear strain (Fig. 9), the equivalent rotational stiffness $K_{e,eq}$, the yield strength $(\Sigma M_y)_{eq}$, and the post-elastic stiffness $K_{p,eq}$ can be established. The analytical predictions correlated well with the available full-scale test results (Fig. 10). The behavior of the dual panel zone can be idealized as that shown in Fig. 11. For an exterior connection (Fig. 3(a)) and interior connection with haunches on both side of the column (Fig. 3(c)), the equivalent rotational stiffness, yield moment and post-elastic stiffness of the dual panel zone is calculated as follows:

3.2.1. Equivalent rotational stiffness

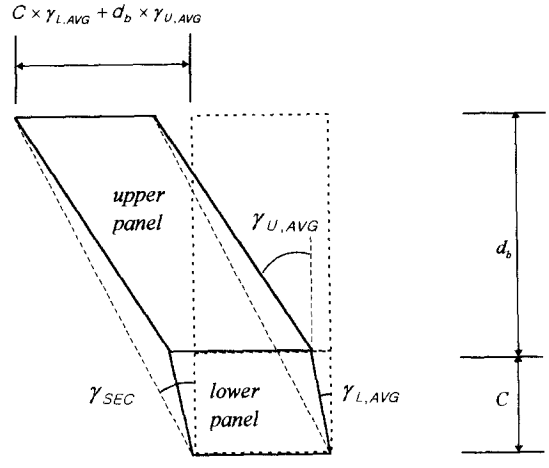

Fig. 9 Deformed configuration of a dual panel zone in shear (Lee-Uang 1997).

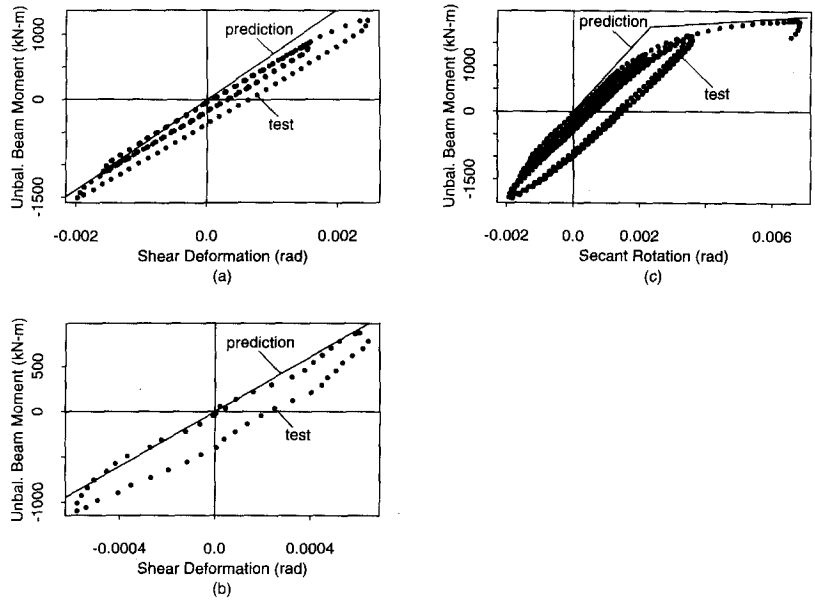

Fig. 10 Prediction versus test results: (a) upper panel zone: (b) lower panel zone; (c) dual panel zone (Lee-Uang 1997).

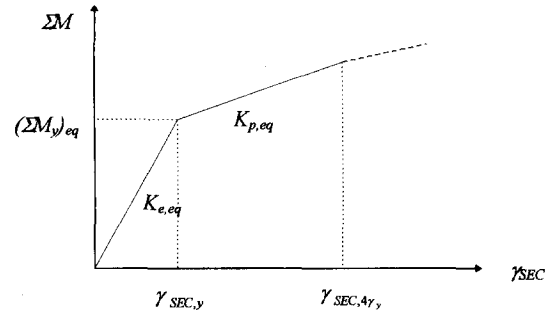

Fig. 11 Unbalanced beam moment versus secant rotation relationship of a dual panel zone.

$$K_{e,eq} = \frac{\alpha_U}{\left(\frac{d_b}{d_b + C}\right)\left(\frac{C}{d_b}\frac{\alpha_U}{\alpha_L}\frac{t_{cw,U}}{t_{cw,L}} + 1\right)} K_{0,U} \tag{2}$$

where

$$K_{0,U} = G\,(d_c - t_{cf})\,t_{cw,U}\,d_b \tag{3}$$

$$\alpha_U = \frac{1}{Q_U\,d_b} \tag{4}$$

$$\alpha_L = \frac{1}{Q_L\,d_b} \tag{5}$$

$$Q_U = \frac{A_{bf} + A_{bw}\,(5 - R_1 R_2)/24}{S_{btf}} - \frac{1}{H_C} \tag{6}$$

$$Q_L = \frac{R_2 A_{hf} + A_{hw}\,(2R_2 + R_1 R_2)/6}{S_{btf}} - \frac{1}{H_C} \tag{7}$$

$$R_1 = \frac{d_b/2}{d_b/2 + C} \tag{8}$$

$$R_2 = \frac{A_{bf} + A_{bw}/4}{R_1(A_{bf} + A_{bw}/4) + (R_1 + 1)A_{hw}/2 + A_{hf}} \tag{9}$$

$$S_{btf} = \frac{d_b\,(1 + R_1 R_2)(6A_{bf} + A_{bw})}{12} + R_2 A_{hf}\left(\frac{d_b}{2} + C\right) + \frac{A_{hw}\,(R_1 R_2 + R_2)}{2}\left[\frac{d_b}{2} + \frac{(R_1 R_2 + 2R_2)}{3(R_1 R_2 + R_2)}\,C\right] \tag{10}$$

See Notations for definitions of the symbols.

3.2.2. Yield moment

$$(\sum M_y)_{eq} = \alpha_U \left(\frac{F_y\,t_{cw,U}\,d_c\,d_b}{\sqrt{3}}\right) \tag{11}$$

3.2.3. Post-elastic stiffness

$$K_{p,eq} = K_p \left(1 + \frac{C}{d_b}\right) \tag{12}$$

where

$$K_p = G \frac{62.4 I_{cf}}{5 t_{cf}} \tag{13}$$

For the dual panel zone of the interior connection with a haunch present on one side of the column only as that shown in Fig. 3(b), Q_U and Q_L defined in Eqs. (14) and (15) should be used instead of those in Eqs. (6) and (7).

$$Q_U = \frac{1}{d_b}\left(1 - \frac{1}{1 + l_{bL}/l_{bR}}\right) + \frac{1}{d_b + C}\left(\frac{1}{1 + l_{bL}/l_{bR}}\right) - \frac{1}{H_C} \tag{14}$$

$$Q_L = \frac{1}{d_b + C}\left(\frac{1}{1 + l_{bL}/l_{bR}}\right) - \frac{1}{H_C} \tag{15}$$

The calculated properties of the dual panel zones based on Eqs. (2)-(15) are summarized in Table 2.

4. Structural characteristics and responses

4.1. Dynamic characteristics

Eigenvalue analysis was performed to study the variations in elastic dynamic characteristics. The "stiffening" effects resulting from the haunch reinforcement decreased the fundamental period by 7%. The fundamental period of the repaired structure was 2.99 seconds and it was still in the "velocity" region of the response spectrum. The changes in natural periods of higher modes were negligibly small. From the viewpoint of design, the repair did not significantly change the design seismic forces.

Table 2 Calculation of dual panel zone properties

(a) Interior connecton with haunches on both sides

Floor (1)	$t_{cw,L}$ (in) (2)	$t_{cw,U}$ (in) (3)	$K_{e,eq}$ (k-in) (4)	$(\Sigma M_y)_{eq}$ (k-in) (5)	$K_{p,eq}$ (k-in) (6)	Hardening (7)
4	1.77	2.77	32,358,845	88,036	2,394,842	.074
3	1.875	2.875	34,304,586	93,272	2,742,644	.08
1	2.19	3.19	40,719,913	112,787	3,629,048	.089

(b) Interior connection with haunch on one side only

Floor (1)	$t_{cw,L}$ (in) (2)	$t_{cw,U}$ (in) (3)	$K_{e,eq}$ (k-in) (4)	$(\Sigma M_y)_{eq}$ (k-in) (5)	$K_{p,eq}$ (k-in) (6)	Hardening (7)
7	1.41	2.785	32,176,708	70,674	1,481,381	.046
6	1.41	2.785	32,414,822	71,078	1,478,432	.046
5	1.77	2.77	34,689,959	75,526	2,394,842	.069
3	1.875	2.875	36,547,149	80,018	2,742,644	.075
2	1.875	2.875	36,547,149	80,018	2,742,644	.075
1	2.19	3.19	42,746,795	97,463	3,629,048	.085

4.2. Inelastic static (push-over) analysis

Inelastic static (push-over) analysis was conducted in order to (1) compute the structure's ultimate strength and (2) predict the yield mechanism (or the potential for a weak story formation) due to repairs. The UBC (1994) lateral load pattern was applied monotonically for the analysis.

4.2.1 Global response

Fig. 12 shows the global response, in the form of base shear ratio versus roof drift ratio, of the original and repaired structures. The elastic lateral stiffness and ultimate strength of the repaired structure were 10% higher than those of the original structure. Structural overstrength of the repaired structure was estimated to be about two at first yield and nearly three at the ultimate level. Distributions of story drift along the building height are summarized in Fig. 13, showing the potential weak stories predicted by the push-over analysis. The plastification occurred mainly between the second and seventh stories. The two structures showed the same weak story mechanism. The differences between the global responses of the original and repaired structures seemed to be slight.

4.2.2. Plastic rotation distribution

Plastic hinging occurred in either the panel zones, columns, or beams away from the face of the column (i.e., the shallow end of the haunch). Figs. 14 and 15 show that as a result of the repair the maximum plastic rotations and their distribution within the frame changed significantly. At locations with haunch reinforcement, the beam plastic hinge rotations increased significantly while panel zone yielding in those connections was reduced. That is, the plastic rotation demand had been redistributed, to some extent, from panel zones to beams. Like the original structure, the haunch repair did not cause significant hinging in the columns.

4.3. Inelastic dynamic analysis

4.3.1. Input ground motion

The Oxnard and Sylmar records (N-S component) were used as input motions for the inelastic dynamic analysis. See Fig. 16 for the time histories and response spectra. The Oxnard record was retrieved from the accelerograph in the basement of the building. The Sylmar record was a near-field record featuring large acceleration pulses as high as 0.84 g.

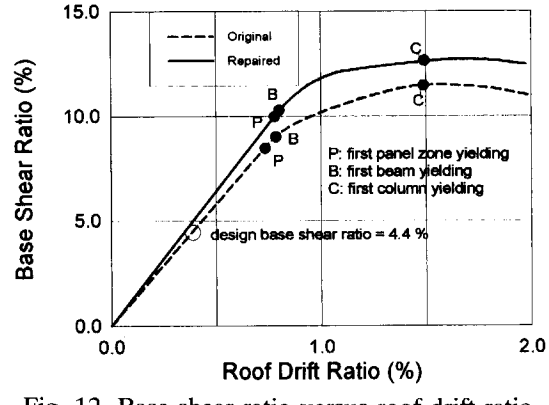

Fig. 12. Base shear ratio versus roof drift ratio.

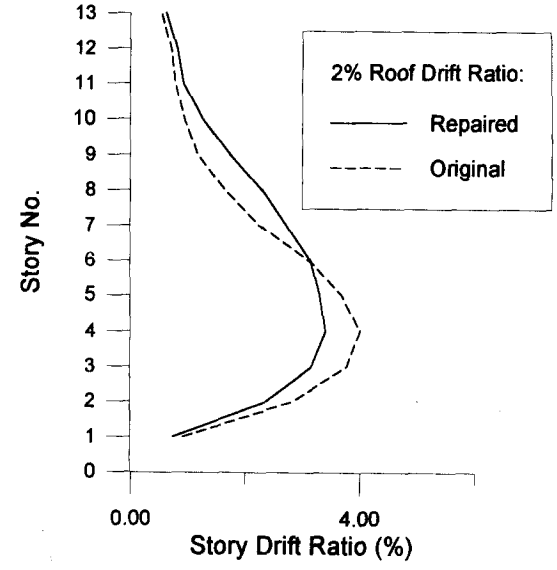

Fig. 13 Story drift distribution along building height.

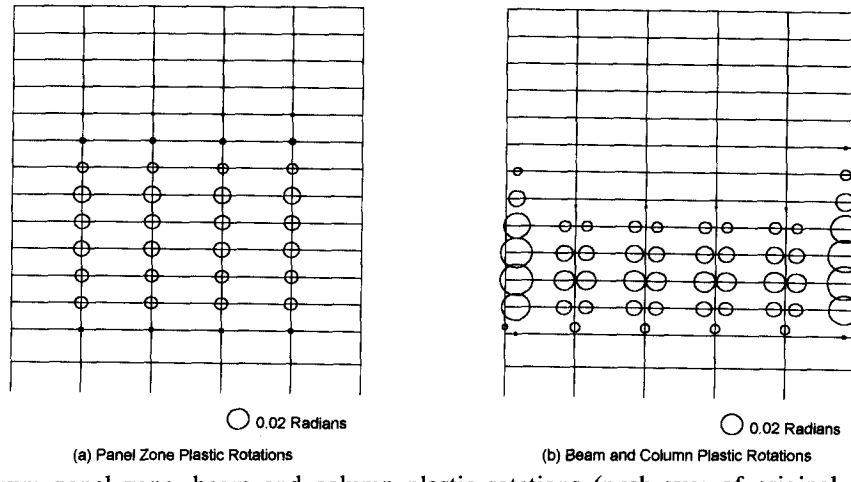

Fig. 14 Maximum panel zone, beam and column plastic rotations (push-over of original model up to 2% roof drift ratio).

4.3.2. Global response

Fig. 17 shows roof displacement responses of the original and repaired structures excited by the Sylmar records. The responses of the two structures were very similar. The response arising from the Sylmar input motion was characterized by two complete cycles of large displacement and subsequent small-amplitude oscillations about a permanent set that formed at the early stage of the ground motion excitation. The response was typical of that arising from near-field, pulse-type excitation. The maximum roof displacement reached twenty-six inches (or a roof drift ratio of 1.25%). The roof displacement responses of the two structures excited by the Oxnard record were also very similar.

Envelopes of story drift ratios by the Sylmar input motion are shown in Fig. 18. This input motion produced a maximum story drift ratio in excess of 2%. The positive maximum value occurred in the bottom (third-fourth) stories and negative minimum value, of similar magnitude.

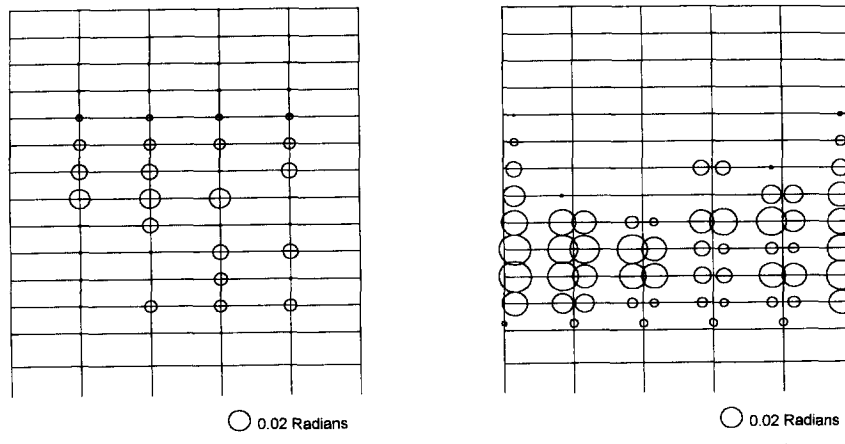

(a) Panel Zone Plastic Rotations (b) Beam and Column Plastic Rotations

Fig. 15 Maximum panel zone, beam and column plastic rotations (push-over of repaired model up to 2% roof drift ratio).

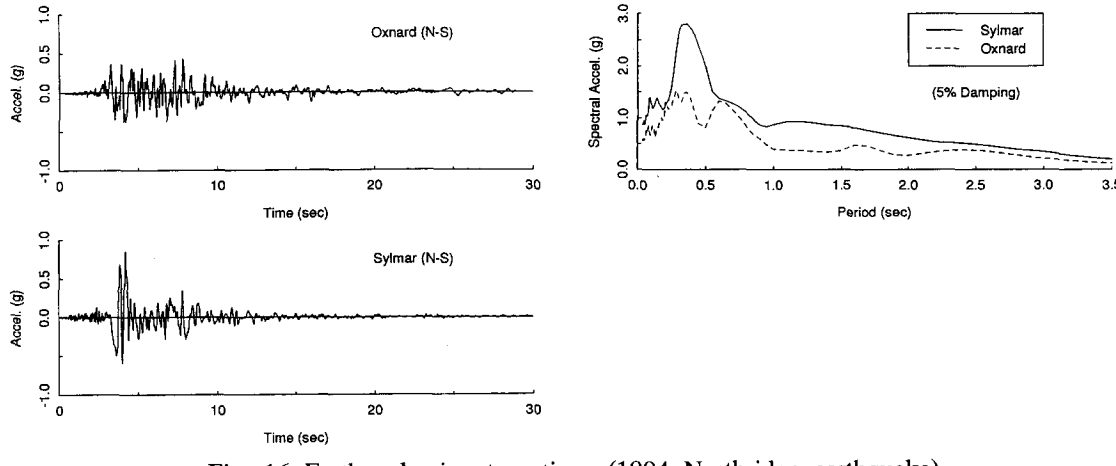

Fig. 16 Earthquake input motions (1994 Northridge earthquake).

also occurred in the upper (eighth-ninth) stories. It is interesting to note that the push-over analysis (Fig. 13) failed to predict the high story drift ratios in the upper stories (Fig. 18). Again, the difference between the global dynamic responses of the original and repaired structures seemed to be small.

4.3.3. Plastic rotation demand

The maximum plastic rotations of panel zones, beams and columns by the Sylmar input motion are shown in Figs. 19 and 20. The patterns of these plastic rotation demands were similar to those obtained from the push-over analysis. That is, at locations repaired with haunches, beam plastic rotations which occurred at the shallow end of the haunch increased while panel zone yielding at those connections was reduced. Nevertheless, the change in maximum magnitude was small and the maximum plastic rotation demands of the repaired structure was virtually equal to those of the original structure. For the original structure, maximum plastic rotation demands of panel zones and beams were 0.012 and 0.015 radians, respectively. For the repaired

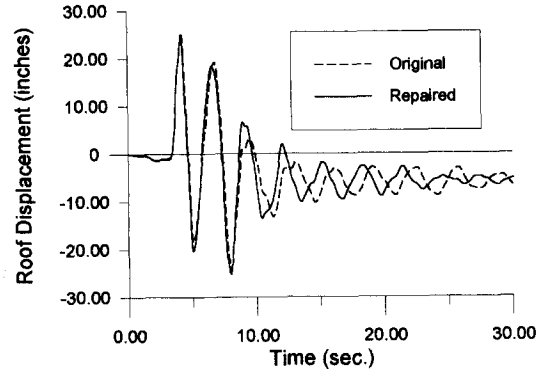

Fig. 17 Roof displacement time histories (Sylmar N-S component).

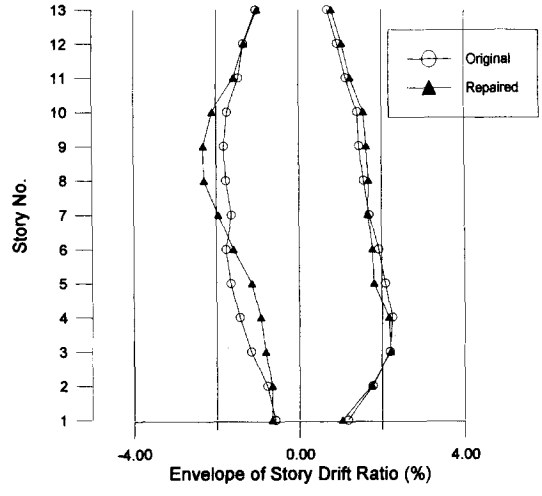

Fig. 18 Story drift distribution along building height (Sylmar N-S component).

structure, maximum plastic rotation demands were 0.013 and 0.017 radians in the panel zones and beams, respectively. The Sylmar record caused very limited column yielding between the plaza level and the second floor of the original structure. The extent of the column yielding was increased after repair, although the plastic rotation demand was still very small.

4.3.4. Distribution of energy dissipation

During a severe earthquake excitation, beams and panel zones in steel MRFs are two major sources of energy dissipation according to the design philosophy. Once a steel frame is repaired with haunches, the panel zones of the strengthened connections are less likely to yield and the distribution of energy dissipation within a structure will be altered.

The energy quantity reflects not only the intensity but also the duration effects of the ground motion. Fig. 21 shows the profiles of the input energy time histories. The repair resulted in about a 20% increase in earthquake energy input for the both records. But the change in overall response seemed to be slight. The input energy time history produced by the Sylmar record showed a large energy power featuring its pulse-type nature as a near-field motion (see Fig. 16). This analysis also indicates that the earthquake input energy produced by the Sylmar record was about two times that of the Oxnard record.

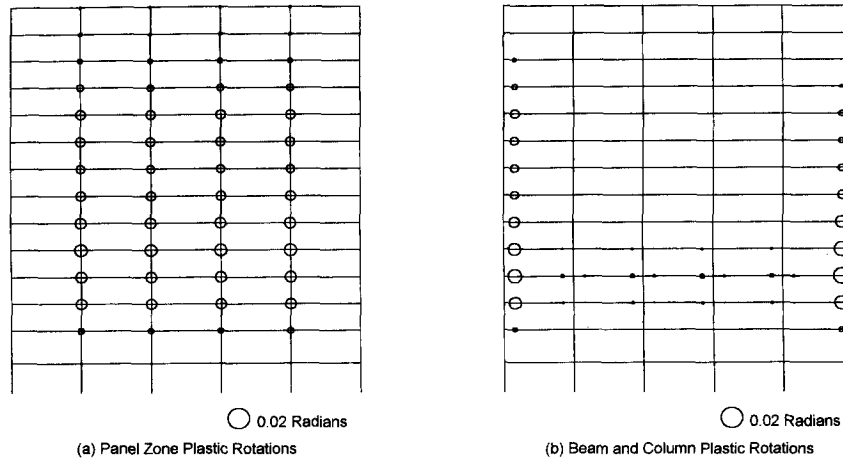

Fig. 19 Maximum panel zone, beam and column plastic rotations (response of original model to Sylmar N-S record).

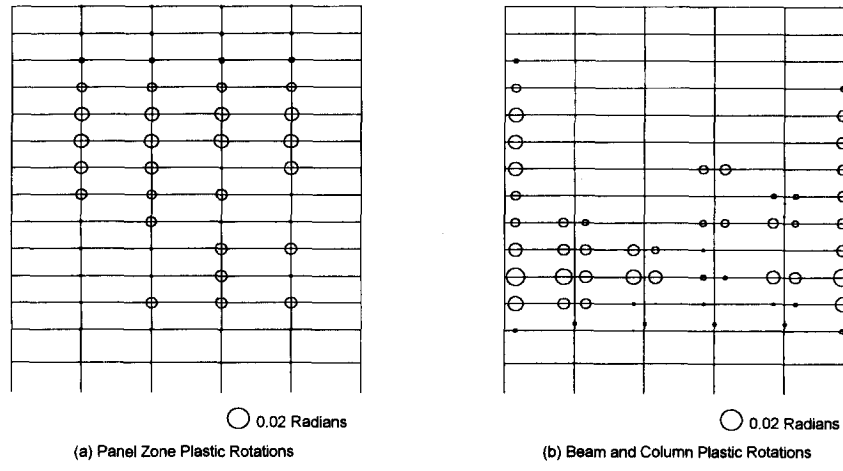

Fig. 20 Maximum panel zone beam and column plastic rotations (response of repaired model to Sylmar N-S record).

The relative distributions of the absorbed energy (or elasto-plastic work) in the original and repaired structures are compared component-wise in Fig. 22. It is clear that the repair drastically shifted the absorbed energy demand from panel zones to beams. In the original structure, panel zones should absorb and dissipate about 80% (for the Oxnard record) and 70% (for the Sylmar record) of the total absorbed energy. But in the repaired structure the panel zones and beams shared almost an equal amount.

5. Summary and conclusions

Based on the results of inelastic static and dynamic analyses of a 13-story steel moment-resisting frame, the effects on the seismic response of a repair scheme which uses haunches to reinforce damaged connections can be summarized as follows.

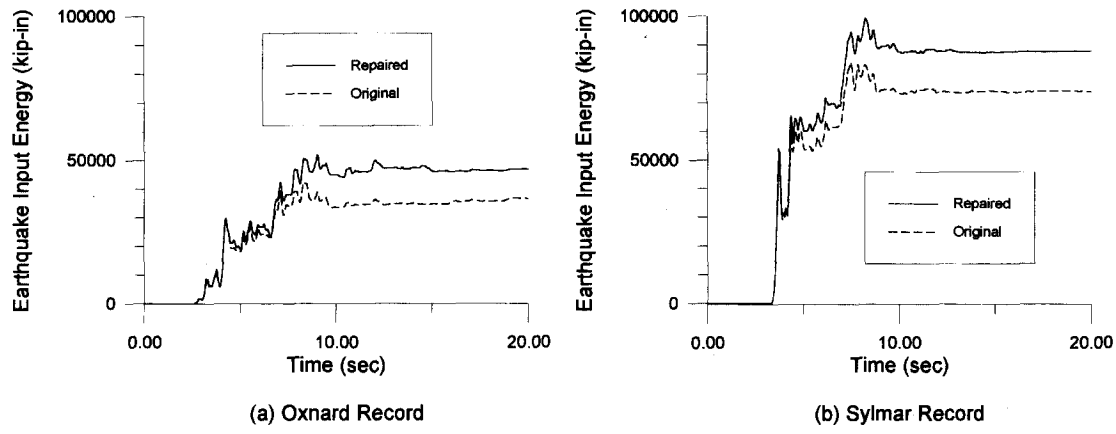

Fig. 21 Input energy time histories.

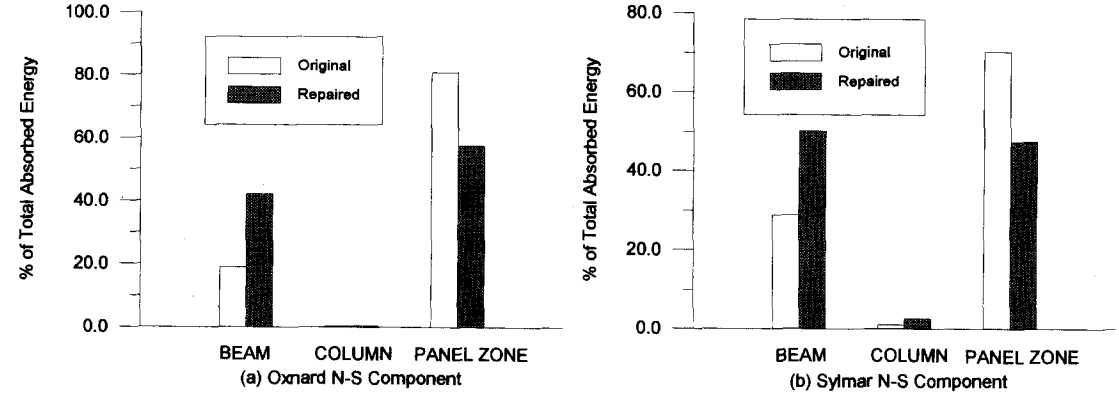

Fig. 22 Distribution of energy dissipation in structures.

(1) The presence of haunches on either or both sides of a connection significantly increases the stiffness and strength of the panel zone and should properly be considered in the analysis. The modeling procedure presented in this paper can be used for an analytical prediction of the seismic performance of multistory steel moment frames when haunches are used to repair damaged steel moment frames as well as to strengthen existing and new steel construction.

(2) Both static and dynamic analysis showed that the global responses of the original and repaired structures were very similar. As a result of adding haunches to the damaged connections, the increases in elastic lateral stiffness and ultimate strength were about 10%. The resulting overstrength of the repaired structure at ultimate level was about three times the 1994 UBC design base shear level. The elastic dynamic characteristics of the repaired structure remained almost the same as those of the original structure and the two structures showed almost identical roof displacement responses for the Oxnard and Sylmar input ground motions.

(3) Both the original and repaired structures showed a similar story drift profile and yielding mechanism, that is, the repair did not trigger an undesirable weak story mechanism.

(4) Following the SAC Interim Guidelines, the haunches thus designed effectively pushed plastic hinging away from the column face. The presence of haunches on either or both sides of a connection significantly changed the distributions of plastic rotation demand in the beams and panel zones. For those connections repaired with haunches, beam plastic rotations were in-

creased to compensate for the reduced plastic rotation demand in the panel zones. But the maximum plastic rotations in the repaired structure were virtually equal to those in the original structure.

(5) The repair resulted in a minor increase in earthquake energy input, but the overall profiles of the input energy time histories did not change. The presence of haunches drastically changed the distribution of energy dissipations among the structural components. In the original structure, panel zones should dissipate about 80% (for the Oxnard record) and 70% (for the Sylmar record) of the absorbed energy. After repairs, the panel zones and beams dissipated a similar amount of energy.

Acknowledgements

The author would like to express his special gratitude to Professor C. M. Uang for providing guidance to this study during his stay at University of California (San Diego) as a visiting scholar.

References

AISC (1994), Load and Resistance Factor Design Specification for Structural Building (LRFD), American Institute of Steel Construction, Ill.

AISI (1994), "Statistical Analysis of Tensile Data for Wide-Flange Structural Shapes," Univ. of Texas-Austin, *Report to the Steel Shape Producers Council.*

"Interim guidelines: evaluation, repair, modification and design of welded steel moment frame structures." (1995). *Report No. SAC-95-02*, Federal Emergency Management Agency, Sacramento, Calif.

Krawinkler, H. (1978), "Shear in beam-column joints in seismic design of steel frames", *Engineering Journal, AISC*, **15**(3), 82-91.

Lee, C.H. and Uang, C. M. (1995a). "Seismic response of haunch repaired steel SMRFs: analytical modeling and a case study". *Report NO. SSRP 95/11*, Univ. of California, San Diego, Calif.

Lee, C.H. and Uang, C. M. (1995b). "Analytical and field investigations of buildings affected by the Northridge earthquake of January 17, 1994". *Report NO. SAC-95-04, Part 2*, pp. 8-1-8-49, ATC, Redwood City, Calif.

Lee, C.H. and Uang, C. M. (1997). "Analytical modeling of a dual panel zone in haunch repaired steel MRFs". *J. of Struct. Engrg., ASCE*, **123**(1), 20-29.

Prakash V., Powell, G.H. and Campbell, S. (1993), "DRAIN-2DX," Version 1.10, Structural Engineering, Mechanics and Materials, Dept. of Civil Engineering, Univ. of California, Berkeley, *Report No. UCB/SEMM-93/17.*

Uang, C.M. and Bondad, D. (1996a). "Static cyclic testing of pre-Northridge and haunch repaired steel moment connections". *Report No. SSRP-96/02* (Final Report to SAC), Univ. of California, San Diego, Calif.

Uang, C.M. and Bondad, D. (1996b). "Dynamic testing of pre-Northridge and haunch repaired steel moment connections." *Report No. SSRP-96/03* (Final Report to NSF), Univ. of California, San Diego, Calif.

Uang, C.M., Yu, Q.S., Sadre, A., Bonowitz, D. and Youssef, N. (1995). "Performance of a 13-story steel moment-resisting frame damaged in the 1994 Northridge Earthquake". *Report No. SSRP 95/04*, Univ. of California, San Diego, Calif.

Uniform Building Code (1994), Int. Conf. of Bldg. Officials, Whittier, Calif.

Notations

A_{bf} beam flange area;

A_{bw} beam web area;
A_{hf} haunch flange area;
A_{hw} haunch web area;
C depth of haunch;
d_b depth of beam;
d_c depth of column;
E modulus of elasticity of steel;
E_{sh} strain hardening modulus of steel;
F_y yield stress of steel in tension;
G shear modulus of steel;
H_C story height;
I_{cf} moment of inertia of one column flange;
$K_{0,U}$, K_e conventional rotational stiffness of single panel zone;
$K_{e,eq}$ equivalent rotational stiffness of dual panel zone;
K_p post-elastic stiffness of single panel zone;
K_s strain-hardening stiffness of single panel zone;
$K_{p,eq}$ equivalent post-elastic stiffness of dual panel zone;
l_{bL}, l_{bR} span length to the left and to the right of the connection, respectively;
M_n nominal beam moment strength;
M_{pr} probable beam moment strength;
ΣM unbalanced beam moment;
$(\Sigma M)_y$ yield moment of conventional single panel zone ;
$(\Sigma M_y)_{eq}$ yield moment of dual panel zone;
$1/Q_U$, $1/Q_L$ average depth factors for upper and lower panel zone, respectively;
R_1 ratio of beam bottom flange stress to haunch flange stress;
R_2 ratio of haunch flange stress to beam top flange stress;
S_{btf} repaired section modulus for beam top flange at column face;
t_{cf} thickness of column flange;
$t_{cw,L}$ web thickness of lower panel zone including, if any, doubler plates;
$t_{cw,U}$ web thickness of upper panel zone including, if any, doubler plates;
t_{hw} thickness of haunch web;
α_L stiffness and strength modification factor for lower panel zone;
α_U stiffness and strength modification factor for upper panel zone;
$\gamma_{L,AVG}$ average shear strain in lower panel zone;
$\gamma_{U,AVG}$ average shear strain in upper panel zone;
γ_{SEC} secant rotation of dual panel zone;
$\gamma_{SEC,y}$ secant rotation of dual panel zone at first yield;
$\gamma_{SEC,4\gamma y}$ secant rotation of dual panel zone at upper panel deformation of $4\gamma_y$;
γ_y yield shear strain.